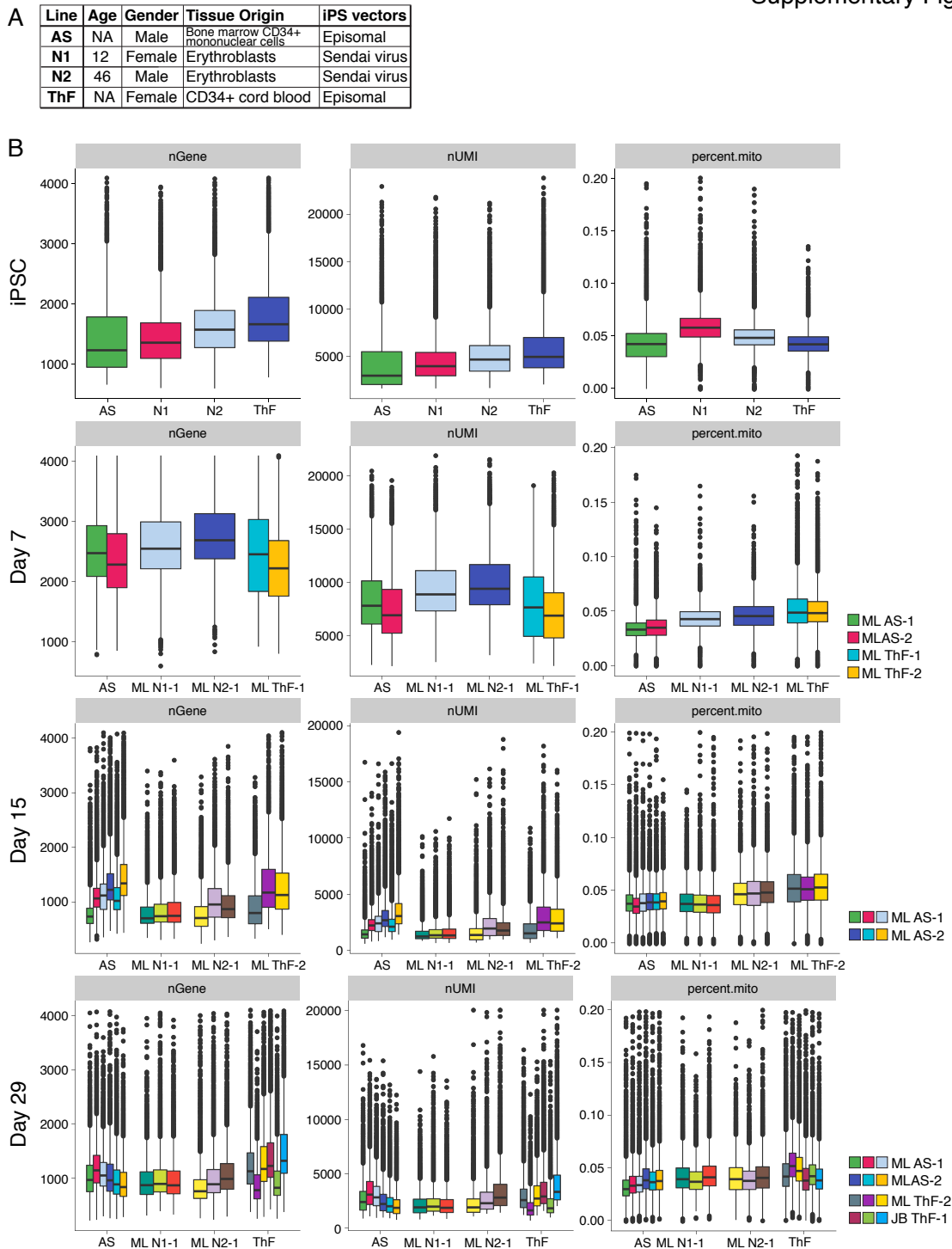
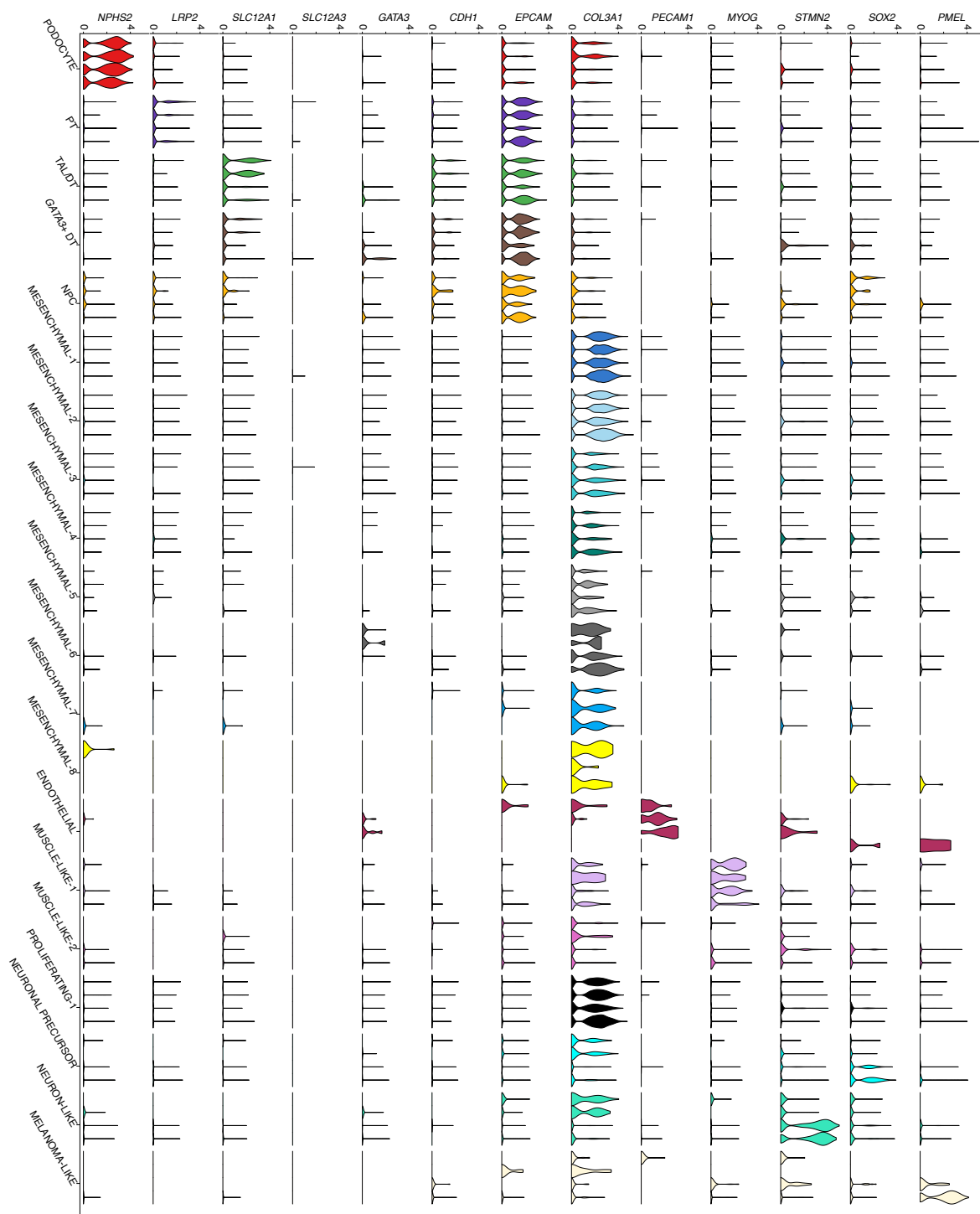


Supplementary Figure 1



Supplementary Figure 1. Data quality metrics for single cell analysis of kidney organoids across four iPSC lines. (A) Table of reference for 4 different iPSC lines. (B) Boxplots of quality control metrics (nGene: number of genes with a normalized expression value above 0 per cell, lower QC cutoff 200; nUMI: the total number of Unique Molecule Identifiers (UMIs) detected per cell, lower QC cutoff 1000; percent.mito: the proportion of reads mapping to mitochondrial genes, upper QC cutoff of 20%) across cell lines and time points. The center line of the boxplots indicates the median, the bottom and top lines of the box indicate the first and third quartiles respectively of the data points. Outliers are indicated as dots beyond the whiskers; whiskers stretch up to $\pm 1.5 \times \text{IQR}$ on both sides. Each data point is a QC measure for a cell.

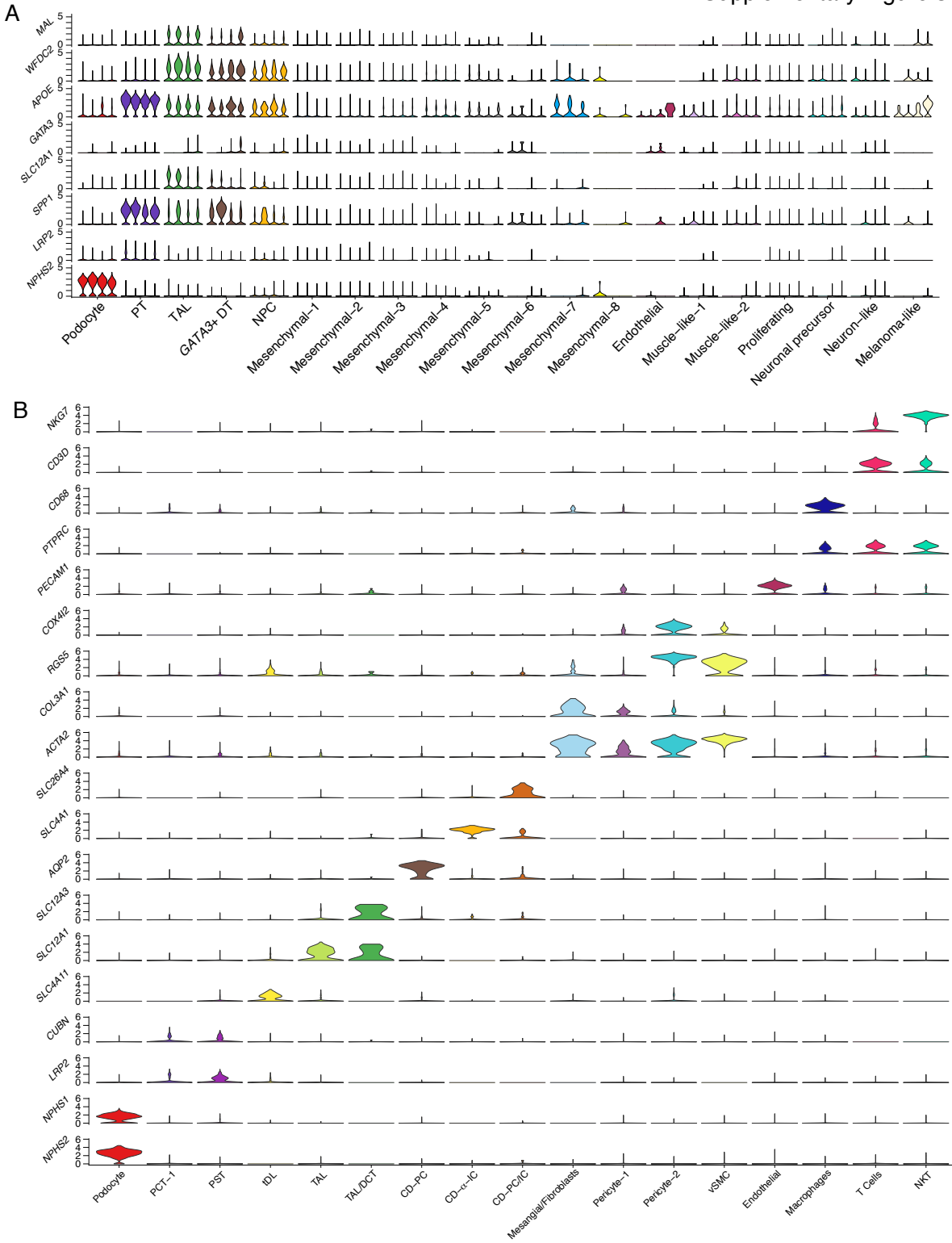
Supplementary Figure 2



Supplementary Figure 2. D29 kidney organoids express canonical markers of major nephron, mesenchymal and off-target cell types.

Violin plots of single cell gene expression from D29 kidney organoids for canonical markers. X-axis annotations represent cell types. Each violin per cell type represents an iPSC line of origin, AS, N1, N2 and ThF in order from left to right. PT, Proximal Tubule; TAL, Thick Ascending Limb; DT, Distal Tubule; NPC, Nephron Progenitor Cell.

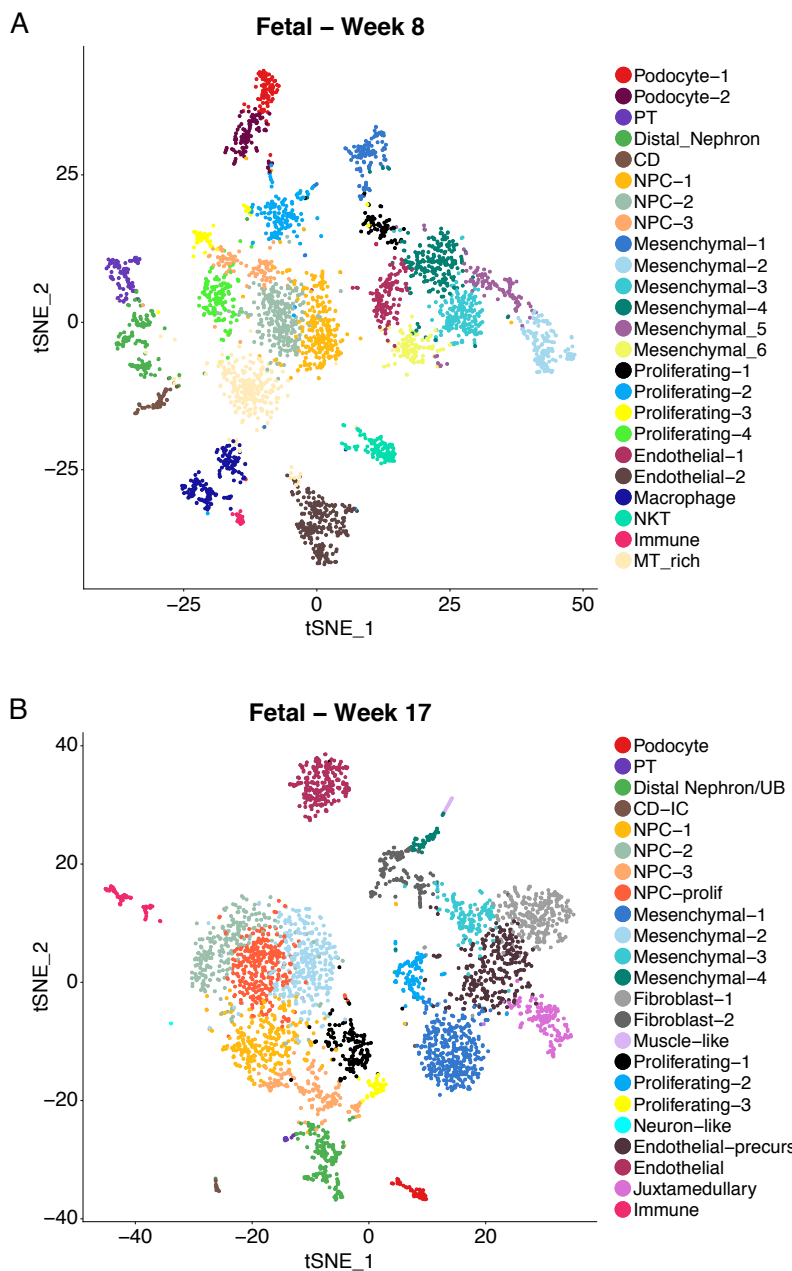
Supplementary Figure 3



Supplementary Figure 3. D29 data-derived markers and canonical markers of major human nephron and kidney cell types.

(A) Violin plots of single cell gene expression from D29 kidney organoids for data-driven markers. X-axis annotations represent cell types. Each violin per cluster represents a line, AS, N1, N2, and ThF in order from left to right. (B) Violin plot of single cell gene expression from human adult nephrectomy for canonical markers. X-axis annotations represent cell types. PCT, Proximal Convolute Tubule; PST, Proximal Straight Tubule; tDL, thin descending limb; DCT, distal convoluted tubule; CD, Collecting Duct; PC, Principal Cell; IC, Intercalated Cell; vSMC, vascular smooth muscle cell; NKT, Natural Killer T cell.

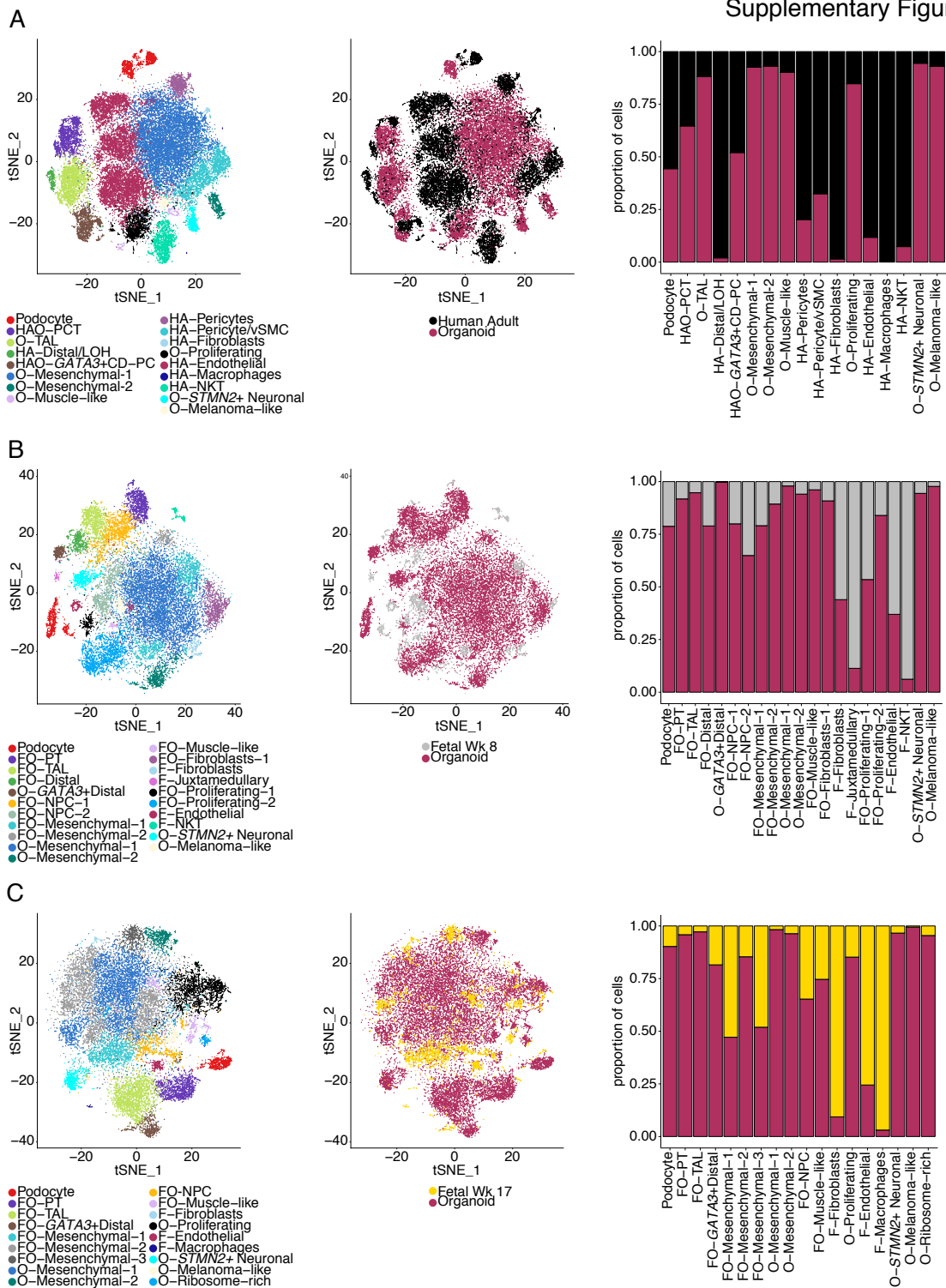
Supplementary Figure 4



Supplementary Figure 4. First and second trimester fetal kidney.

t-SNE plot of single cell transcriptomic profiles from (A) first (Week 8) and (B) second (Week 17) trimester human fetal kidney. Cluster color annotations as shown. MT, mitochondrial. UB, ureteric bud.

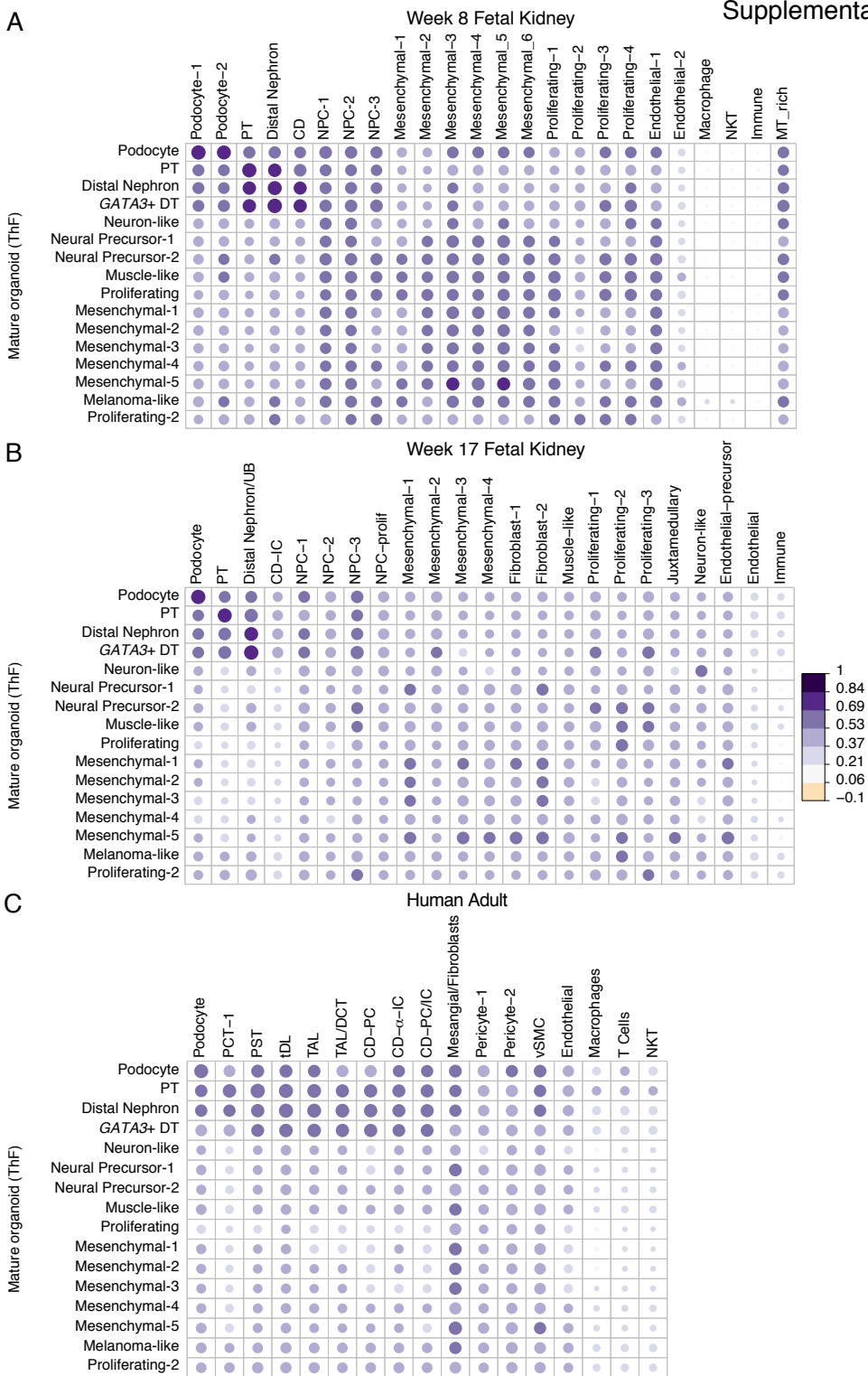
Supplementary Figure 5



Supplementary Figure 5. Integrated analysis of human adult and fetal data with D29 organoids.

Integrated analysis of D29 organoid with (A) human adult and (B) first (Wk 8) and (C) second (Wk 17) trimester fetal kidney data. (Left) t-SNE plot of single cell transcriptomic profiles with cell type color annotations; (Middle) t-SNE plot of single cell transcriptomic profiles with sample origin color annotations; (Right) Proportion plots of sample contribution per cell type. HA, Human Adult; O, Organoid; HAO, well-represented in both human adult and organoid; F, Fetal; FO, well-represented in both fetal and organoid stages.

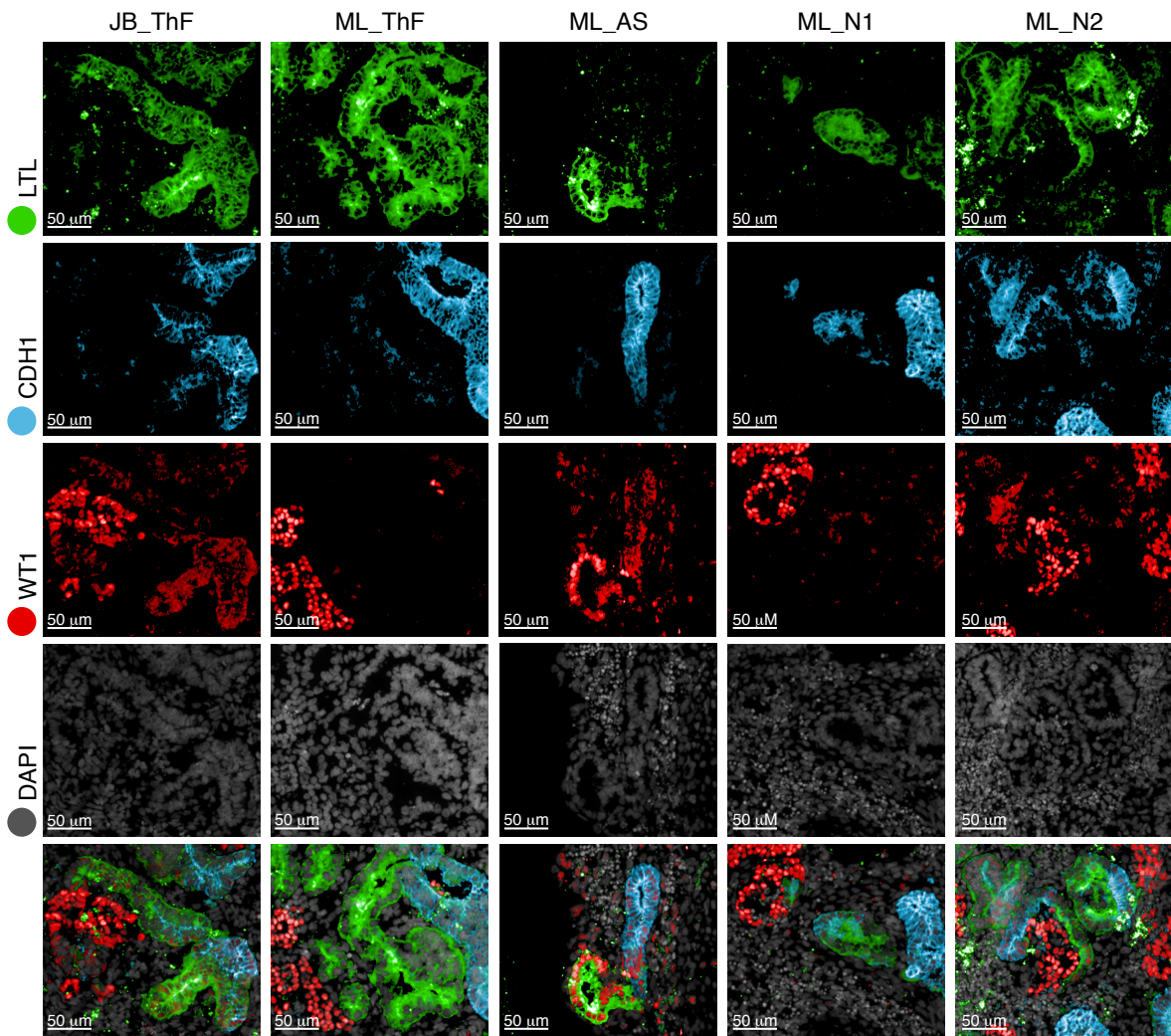
Supplementary Figure 6



Supplementary Figure 6. Spearman correlation between human adult and fetal data versus D29 organoids.

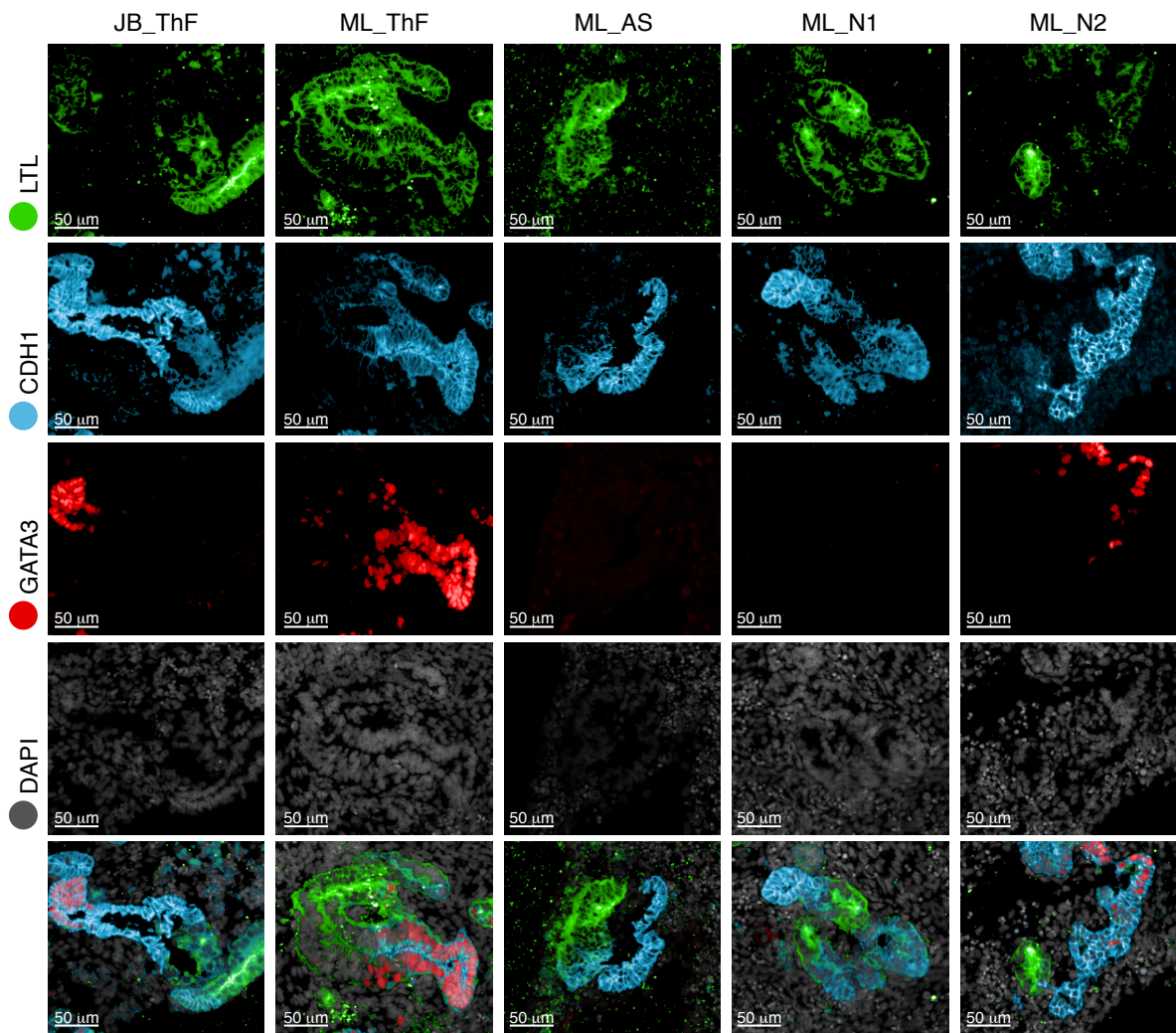
Spearman correlation coefficient of D29 organoid cell types (ThF line) versus (A) first (Wk 8) and (B) second (Wk 17) trimester fetal kidney and (C) human adult clusters.

Supplementary Figure 7



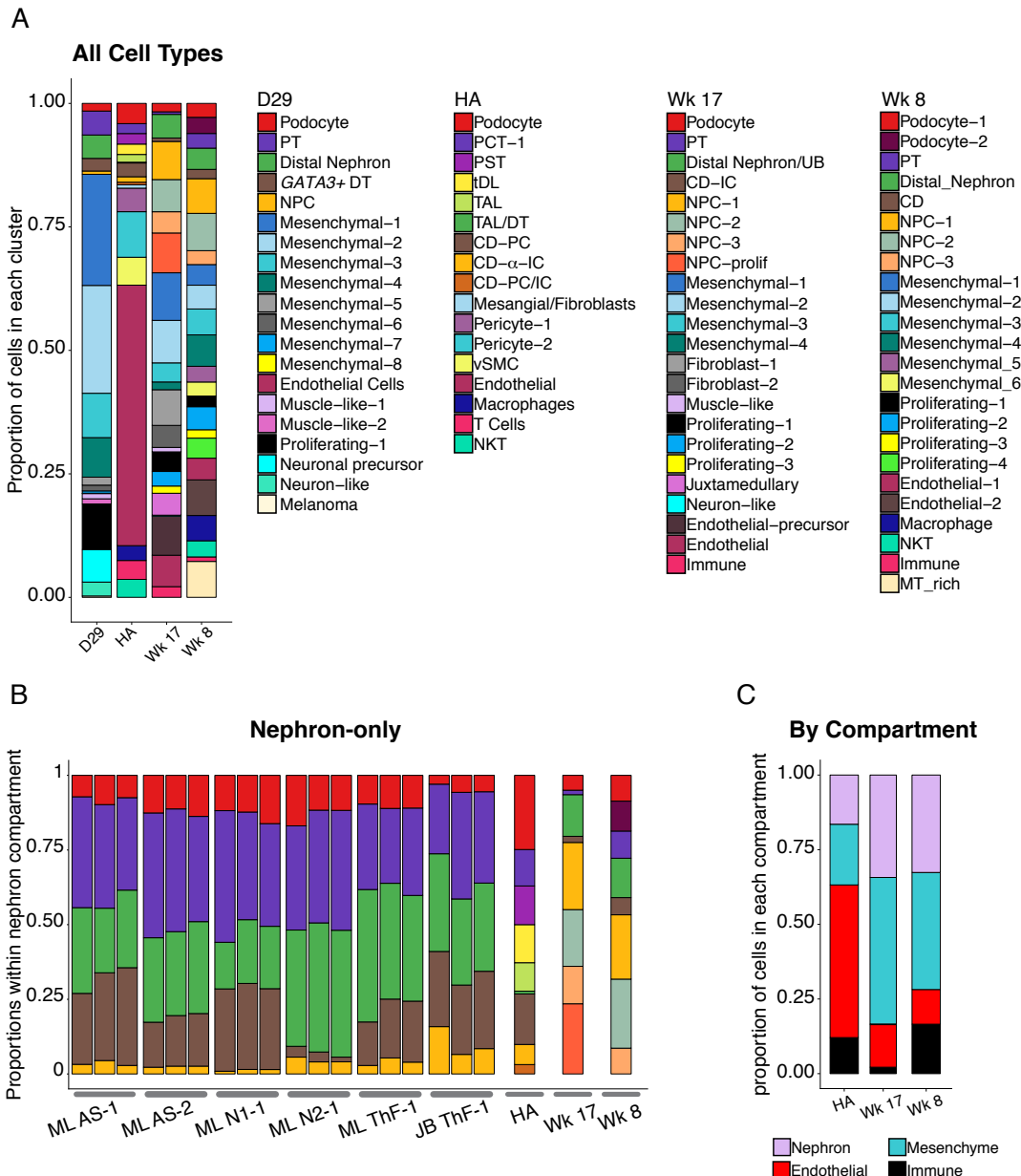
Supplementary Figure 7. Immunofluorescence analysis of D29 kidney organoids demonstrates presence of major nephron cell types from glomerulus to distal tubule. Immunofluorescence staining of D29 kidney organoids for podocytes (WT1), proximal tubular cells (LTL), and the distal tubular compartment (ECAD) across two protocols (JB, ML) and four cell lines (ThF, AS, N1, N2).

Supplementary Figure 8



Supplementary Figure 8. Immunofluorescence analysis of D29 kidney organoids demonstrates presence of major kidney epithelial cell types from proximal to distal tubule.
 Immunofluorescence staining of D29 kidney organoids for proximal tubule (LTL), and distal nephron compartment (ECAD, GATA3) across two protocols (JB, ML) and four cell lines (ThF, AS, N1, N2).

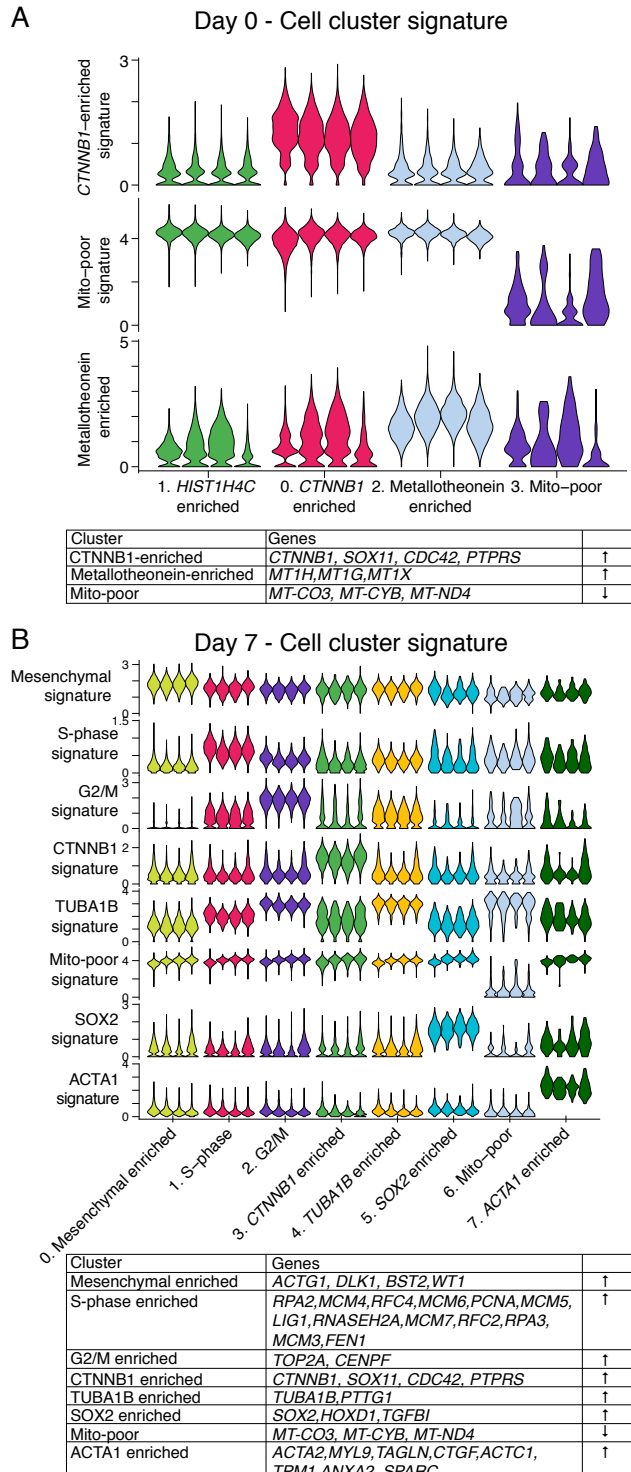
Supplementary Figure 9



Supplementary Figure 9. Cell type proportions of D29 kidney organoids in comparison to human adult and fetal kidneys.

(A) Proportions of cells per cell type averaged across all D29 organoid samples, human adult (HA), and first (Wk 8) and second (Wk 17) trimester fetal kidneys. (B) Proportions of cell classes within the nephron compartment across all lines and replicates at D29, and human adult (HA), and first (Wk 8) and second (Wk 17) trimester fetal kidneys. (C) Proportions of cell compartments across human adult (HA), and first (Wk 8) and second (Wk 17) trimester fetal kidneys.

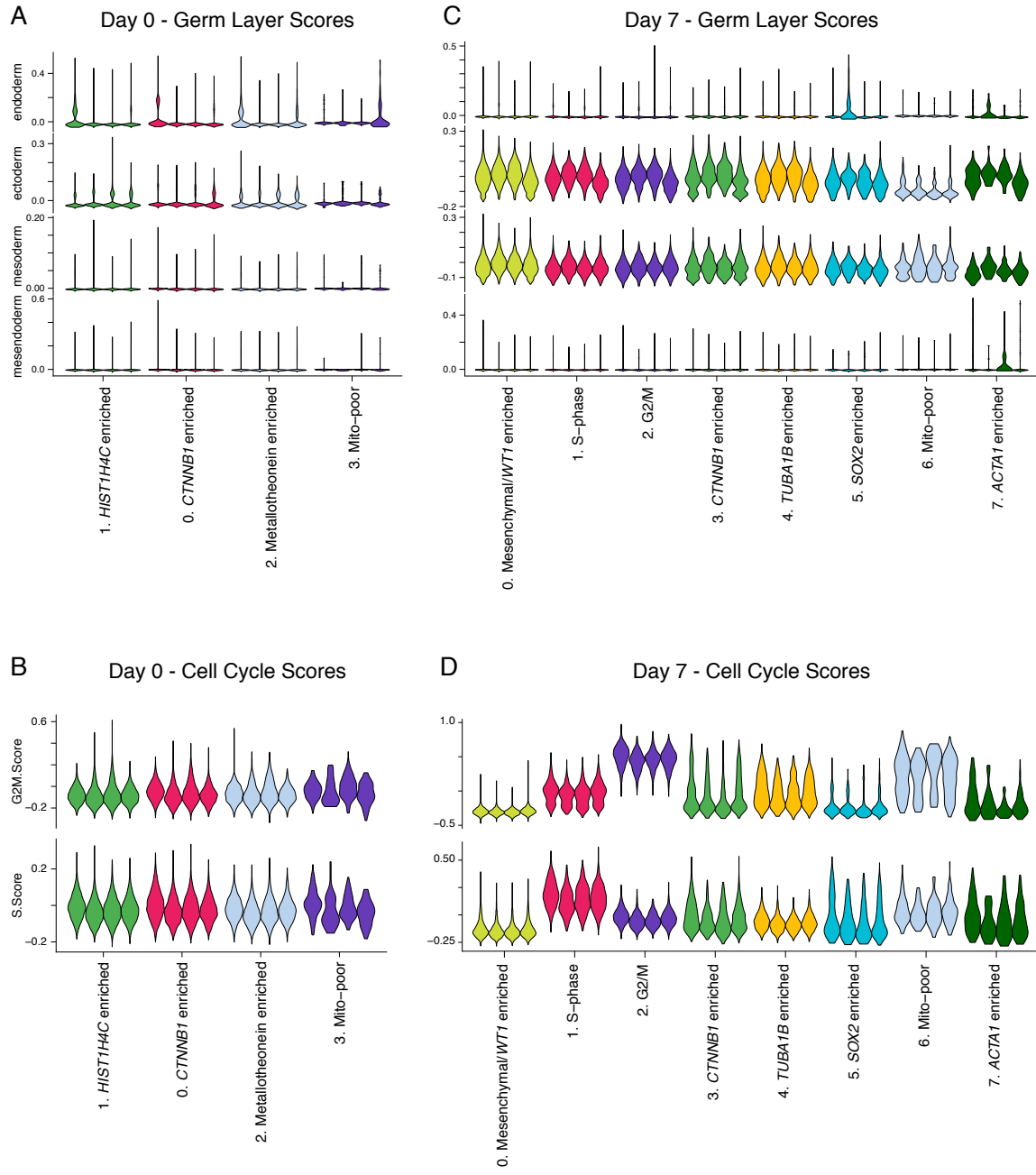
Supplementary Figure 10



Supplementary Figure 10. Cluster specific gene signatures for iPSC D0 and D7 stages

(A) Violin plot of average expression of cluster specific gene signatures in cells in each line at the iPSC stage. Signatures are provided in the table. (B) Violin plot of average expression of cluster specific gene signatures in cells in each line at D7. Signatures are provided in the accompanying table. In each cluster, violins for AS, N1, N2 and ThF are in order from left to right.

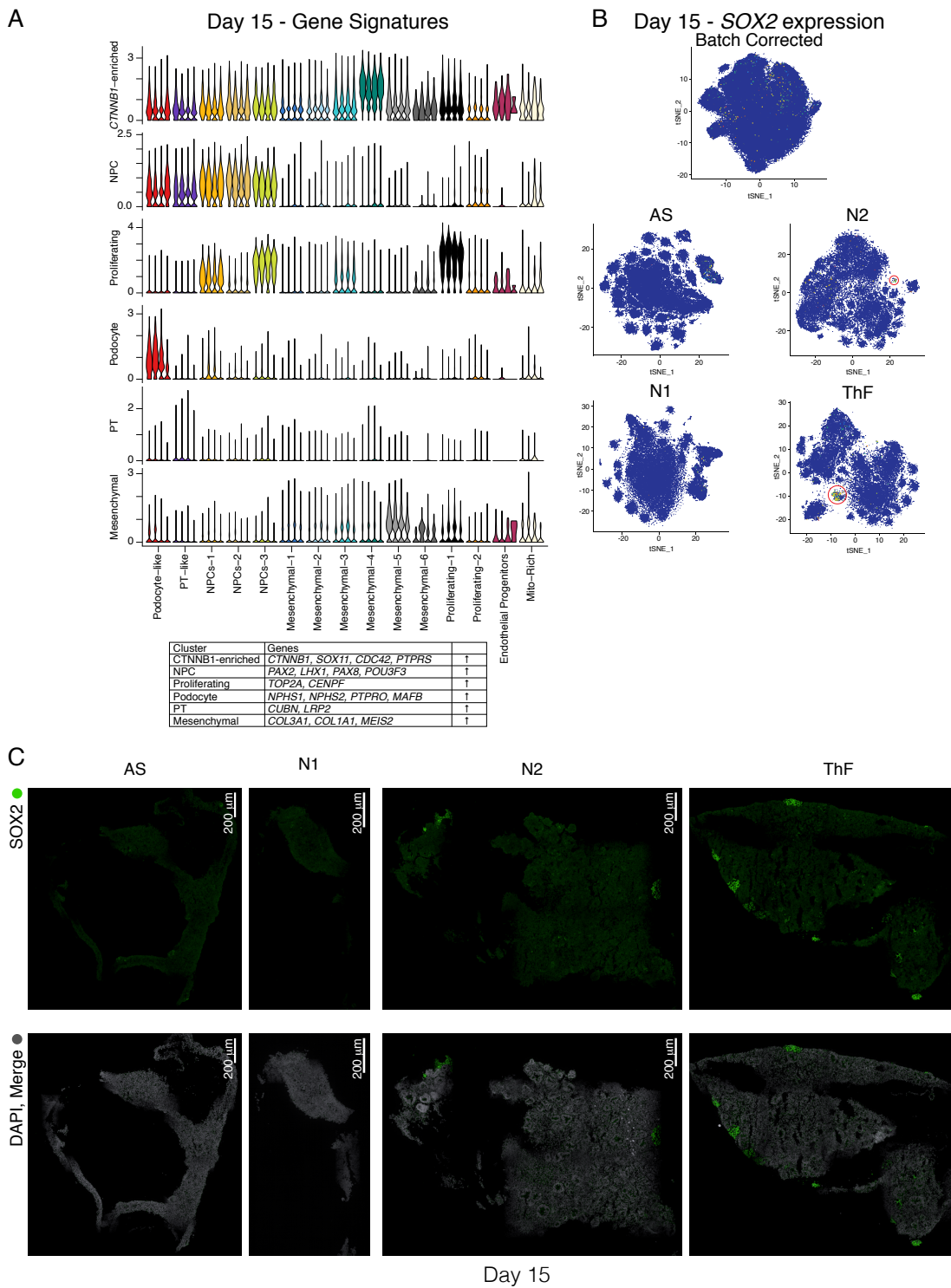
Supplementary Figure 11



Supplementary Figure 11. Single cell analysis of 4 iPSC lines reveals no priming for any specific germ layer and expression of cell-cycle markers.

Violin plot of cluster-specific average expression of germ-layer signatures in single cells from the 4 iPSC lines at (A) D0 and (C) D7. Violin plot of scores for cell cycle phases G2M and S-phase in cells in each iPSC line at (B) D0 and (D) D7 in a cluster specific manner. In each cluster, violins for AS, N1, N2 and ThF are in order from left to right.

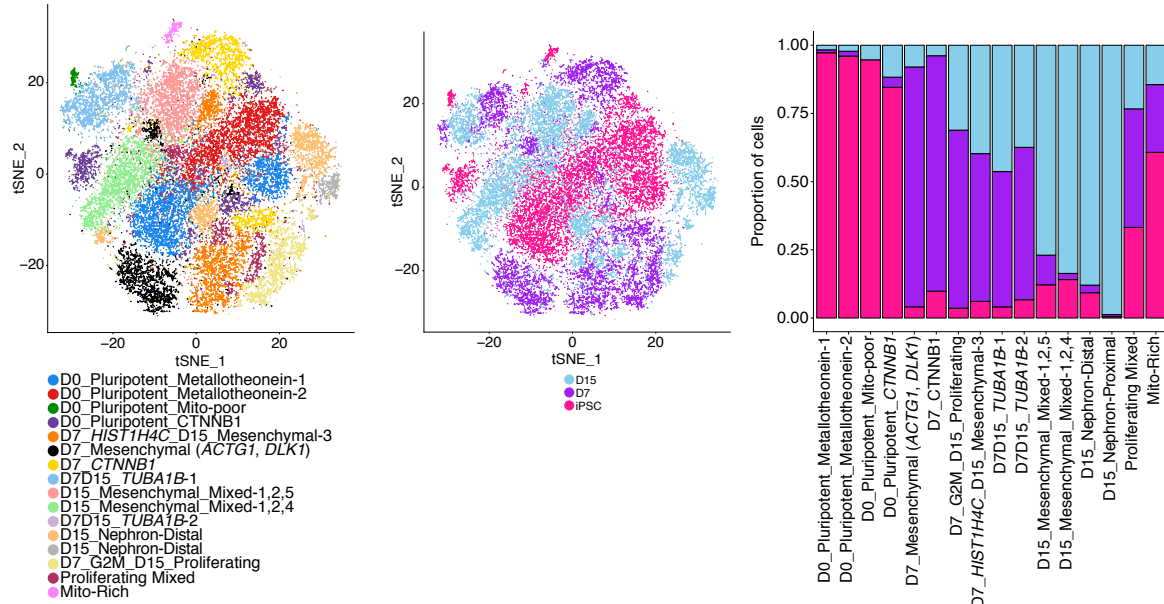
Supplementary Figure 12



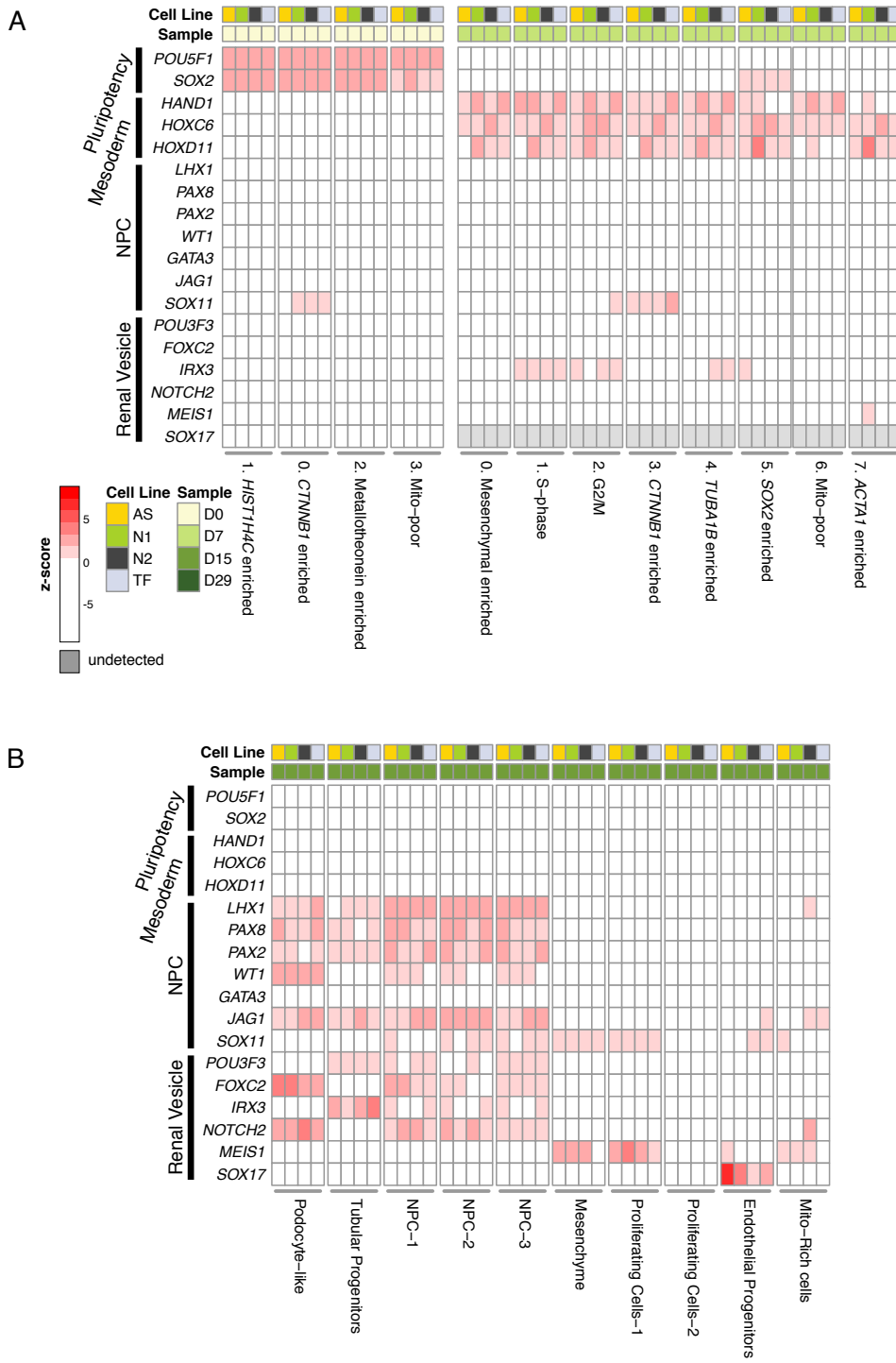
Supplementary Figure 12. Expression of cluster specific gene signatures, line-specific SOX2+ progenitor pools and early markers of podocyte differentiation at D15.

(A) Violin plot of average expression of cluster specific gene signatures in cells in each line at D15 (B) tSNE plot showing variability across the lines in presence of SOX2-positive progenitor cells at D15. Subpopulation of cells (in red circle) expressing SOX2 emerge as early as D15 in ThF and N2. (C) Immunofluorescence staining of D15 kidney organoids for neuron off-target cell populations (SOX2) across four cell lines (AS, N1, N2, ThF).

Supplementary Figure 13



Supplementary Figure 14

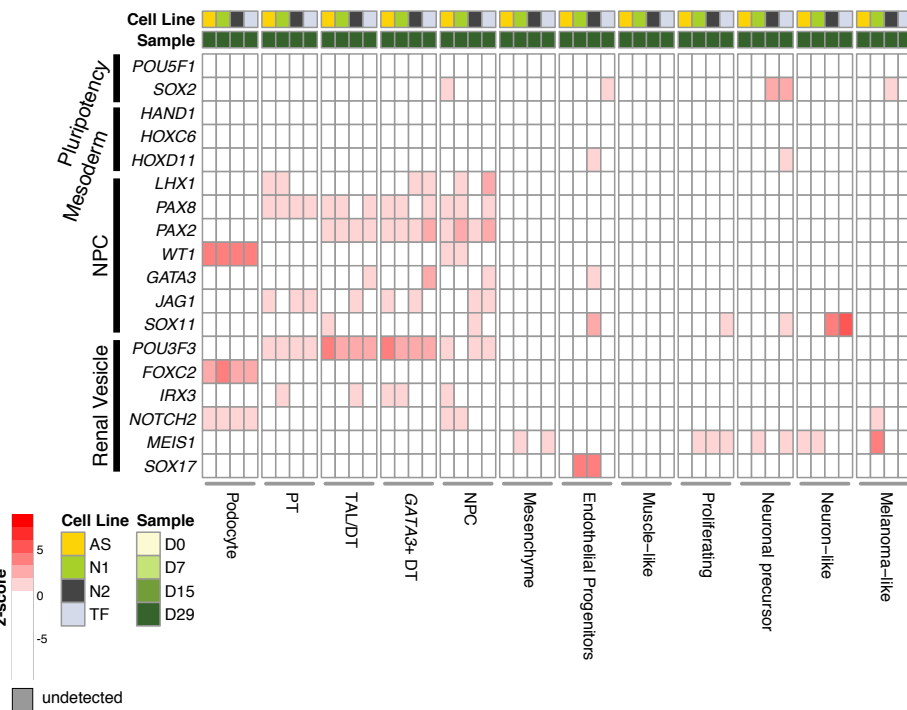


Supplementary Figure 14. Kidney organoid differentiation follows kidney nephrogenesis as determined by expression of transcriptional programs across organoid development time.

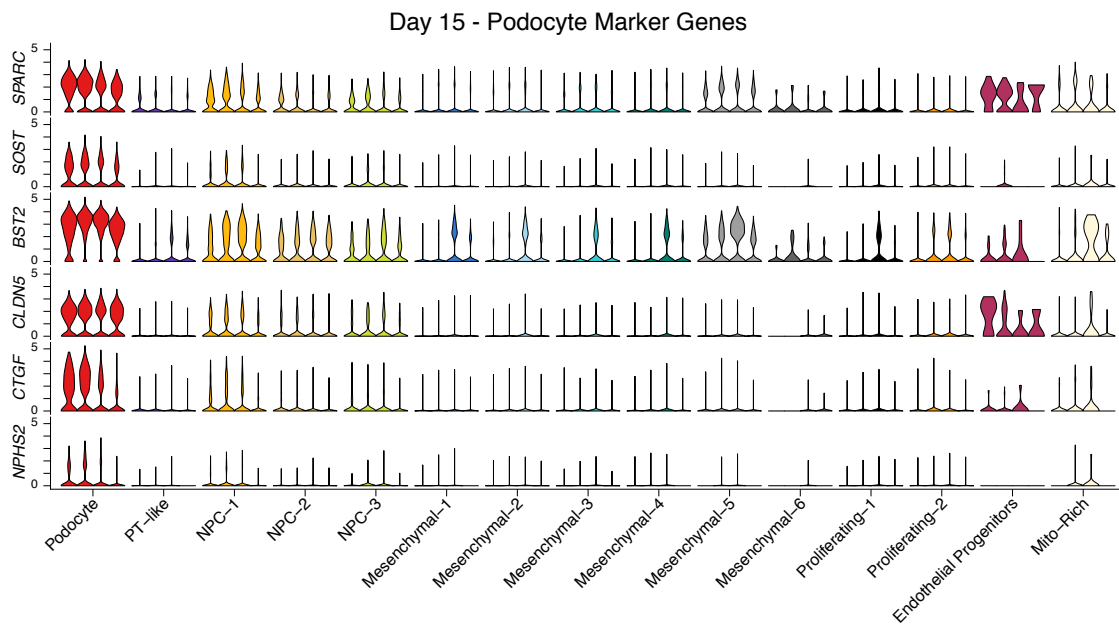
Heat map comparison of expression of major transcription factors and other canonical markers of nephrogenesis across organoid differentiation, (A) iPSC and D7 (B) D15, across the 4 iPSC lines.

Supplementary Figure 15

A



B

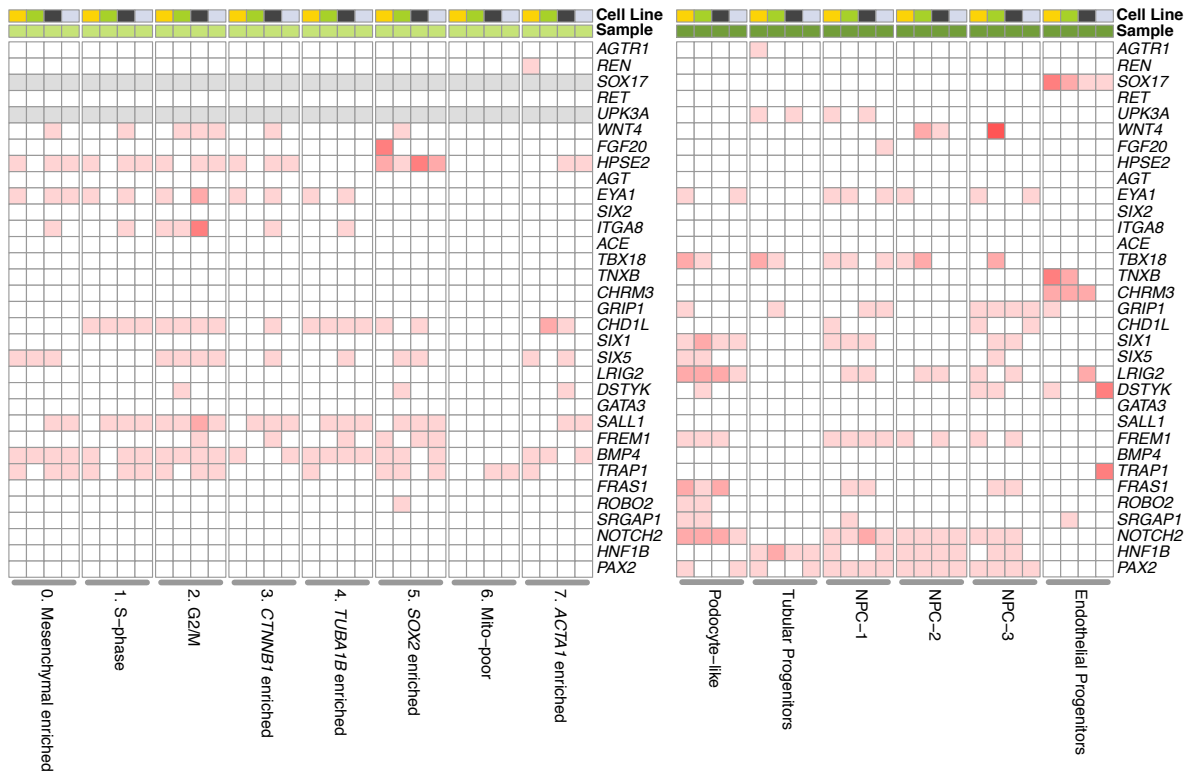


Supplementary Figure 15. Kidney organoid differentiation follows kidney nephrogenesis as determined by expression of transcriptional programs across organoid development time and data-driven podocyte marker genes at D15.

(A) Heat map comparison of expression of major transcription factors and other canonical markers of nephrogenesis in D29 organoids across 4 iPSC lines. (B) Violin plots from D15 organoids for expression of canonical (NPHS2) and data-driven (CLDN5, SOST, BST2, SPARC, CTGF) podocyte marker genes. In each cluster, violins for AS, N1, N2 and ThF are in order from left to right.

Supplementary Figure 16

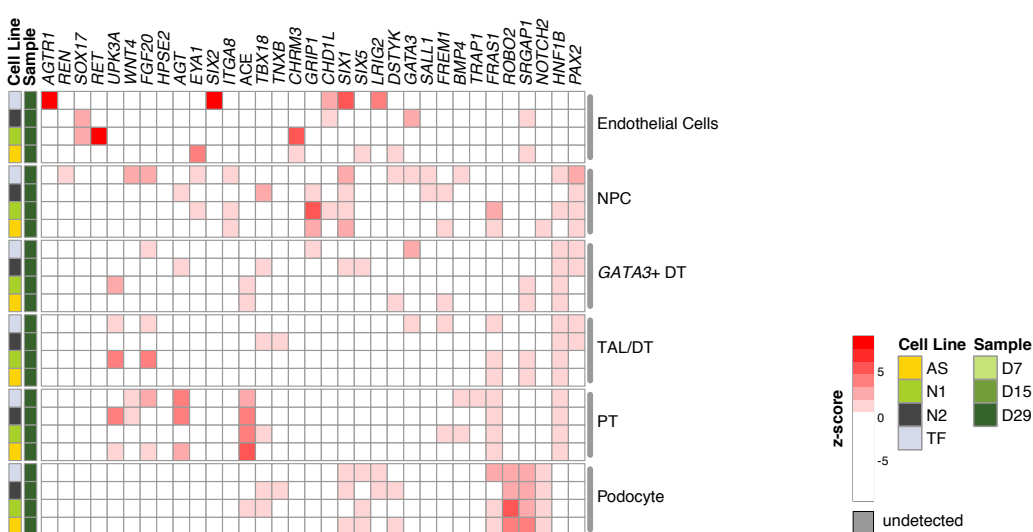
A



B

Endothelial Progenitors

C

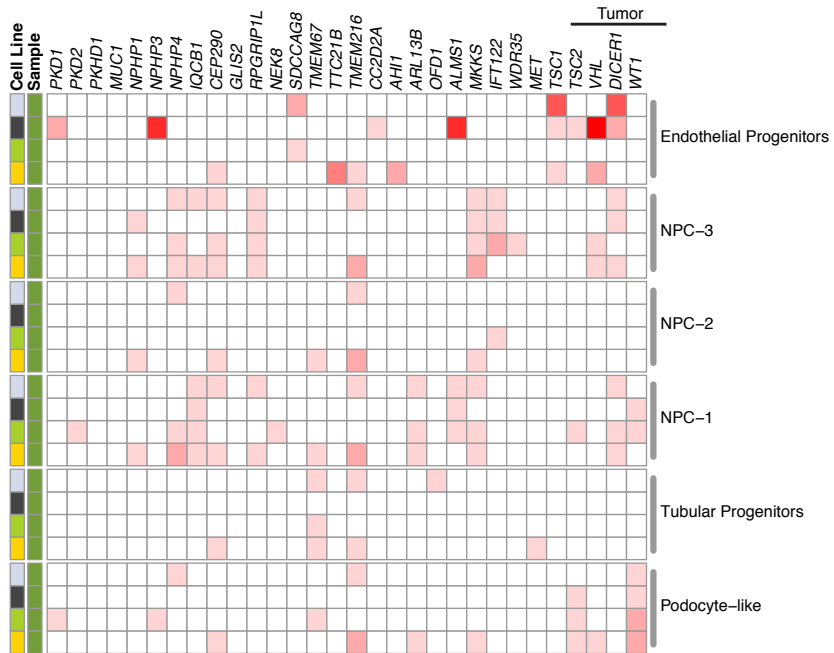
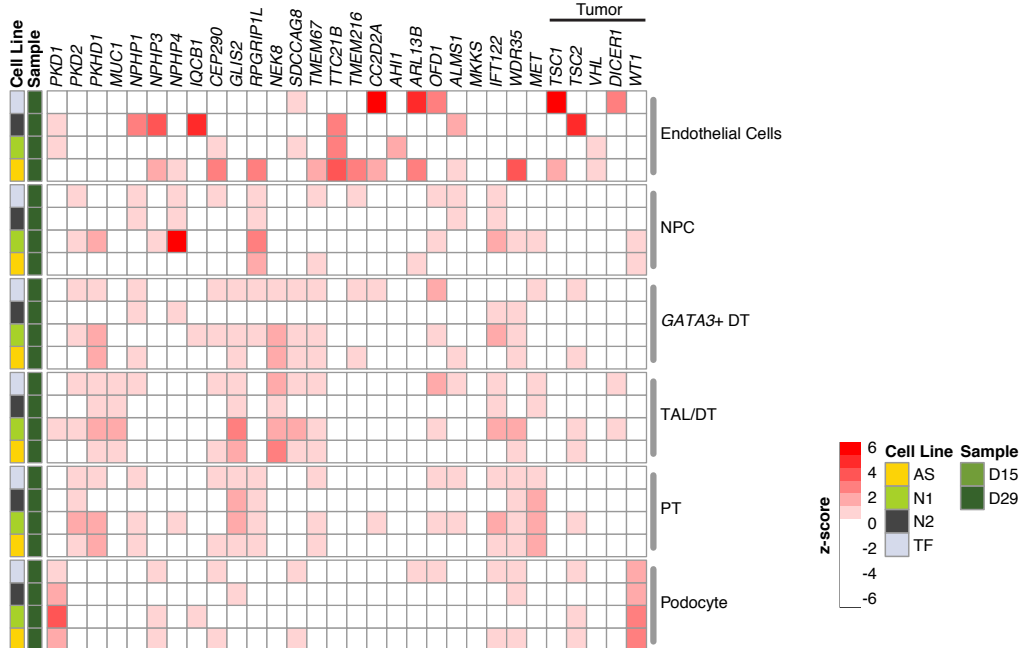


Supplementary Figure 16. Expression of monogenic causes of congenital abnormalities of the kidney and urinary tract (CAKUT) in appropriate nephron epithelial cell types suggests utility of kidney organoids for understanding genetic kidney diseases.

Heat map comparison of gene expression in organoids across differentiation ((A) D7, (B) D15, and (C) D29) of CAKUT-causing genes in kidney epithelial cell clusters (D15, D29) across 4 iPSC lines.

Supplementary Figure 17

Mendelian Cystic Diseases & Tumor Syndromes

A**B**

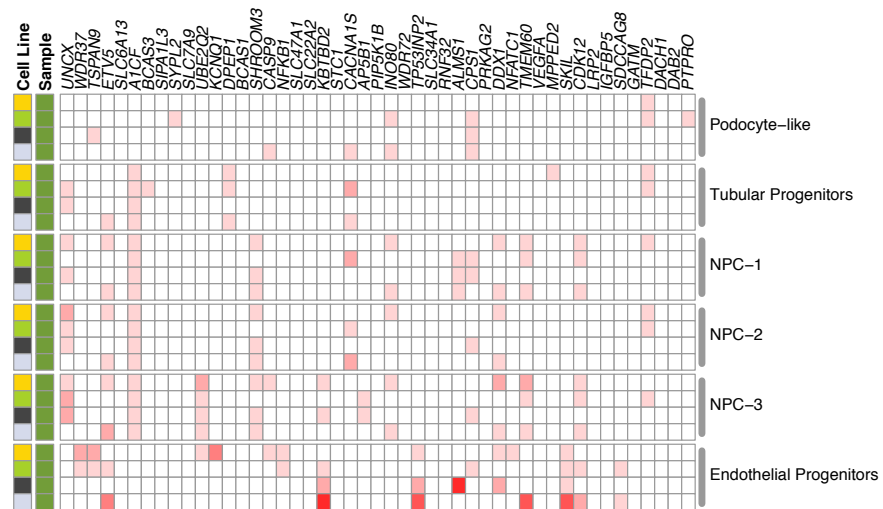
Supplementary Figure 17. Expression of monogenic causes of hereditary renal cystic (HRC) diseases and tumor syndromes in appropriate nephron epithelial cell types suggests utility of kidney organoids for understanding genetic kidney diseases.

Heat map comparison of gene expression in organoids (A) D15, (B) D29 of HRC and tumor syndrome diseases-causing genes in kidney epithelial cell clusters across 4 iPSC lines.

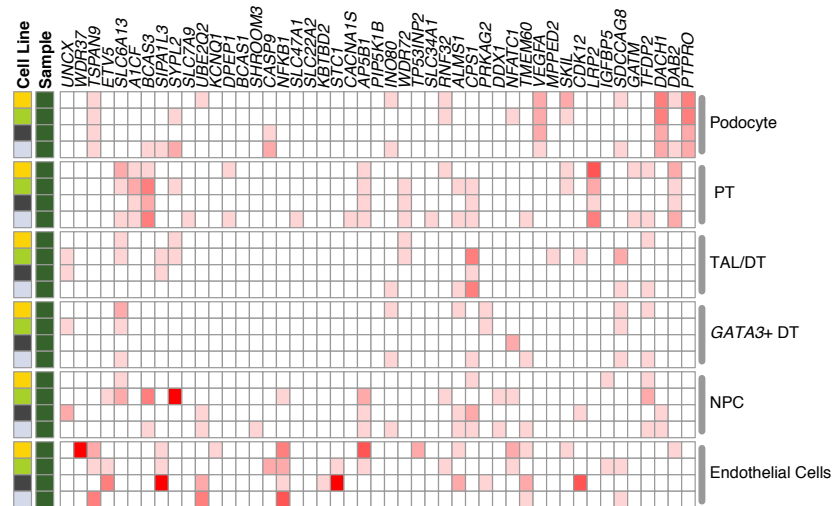
CKD GWAS

Supplementary Figure 18

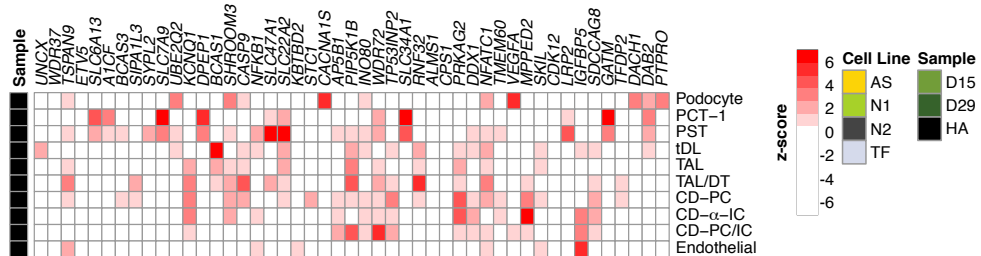
A



B



C



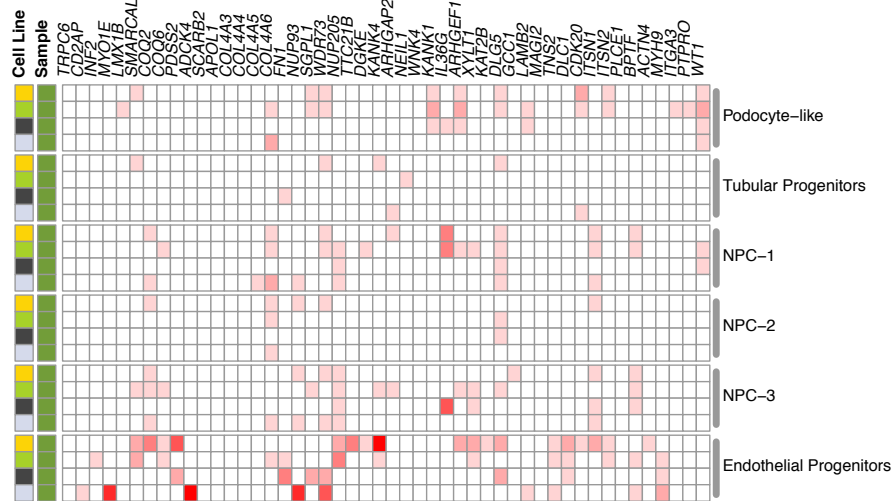
Supplementary Figure 18. Expression of genes associated with chronic kidney diseases (CKD) in appropriate nephron epithelial cell types suggests utility of kidney organoids for understanding genetic kidney diseases.

Heat map comparison of gene expression in organoids ((A) D15, (B) D29) and (C) human adult of genes associated with chronic kidney disease in kidney epithelial cell clusters across 4 iPSC lines.

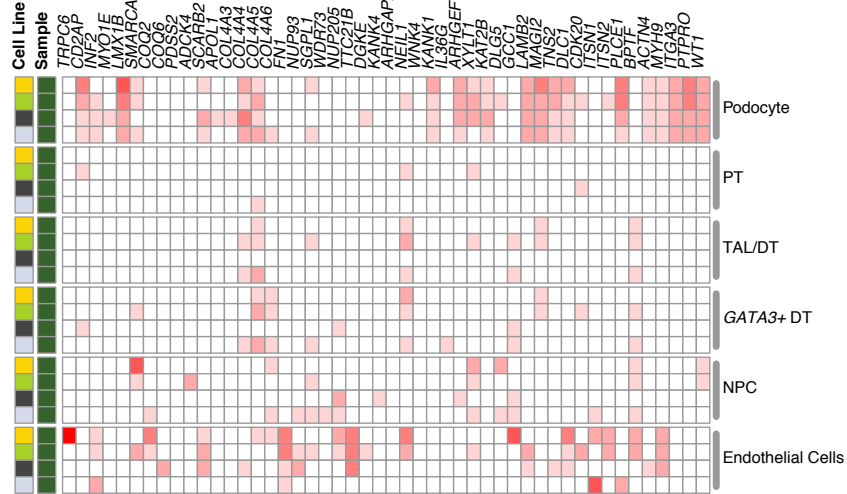
Mendelian Glomerular Diseases

Supplementary Figure 19

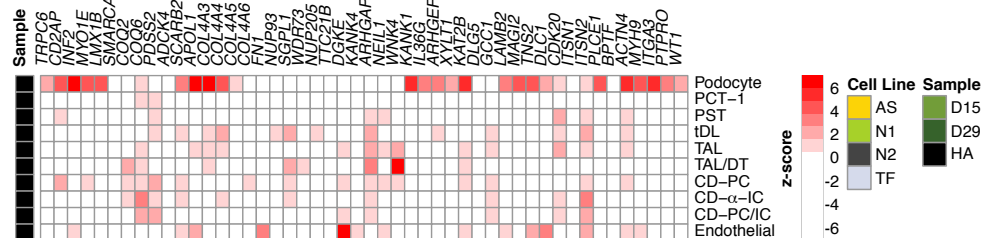
A



B



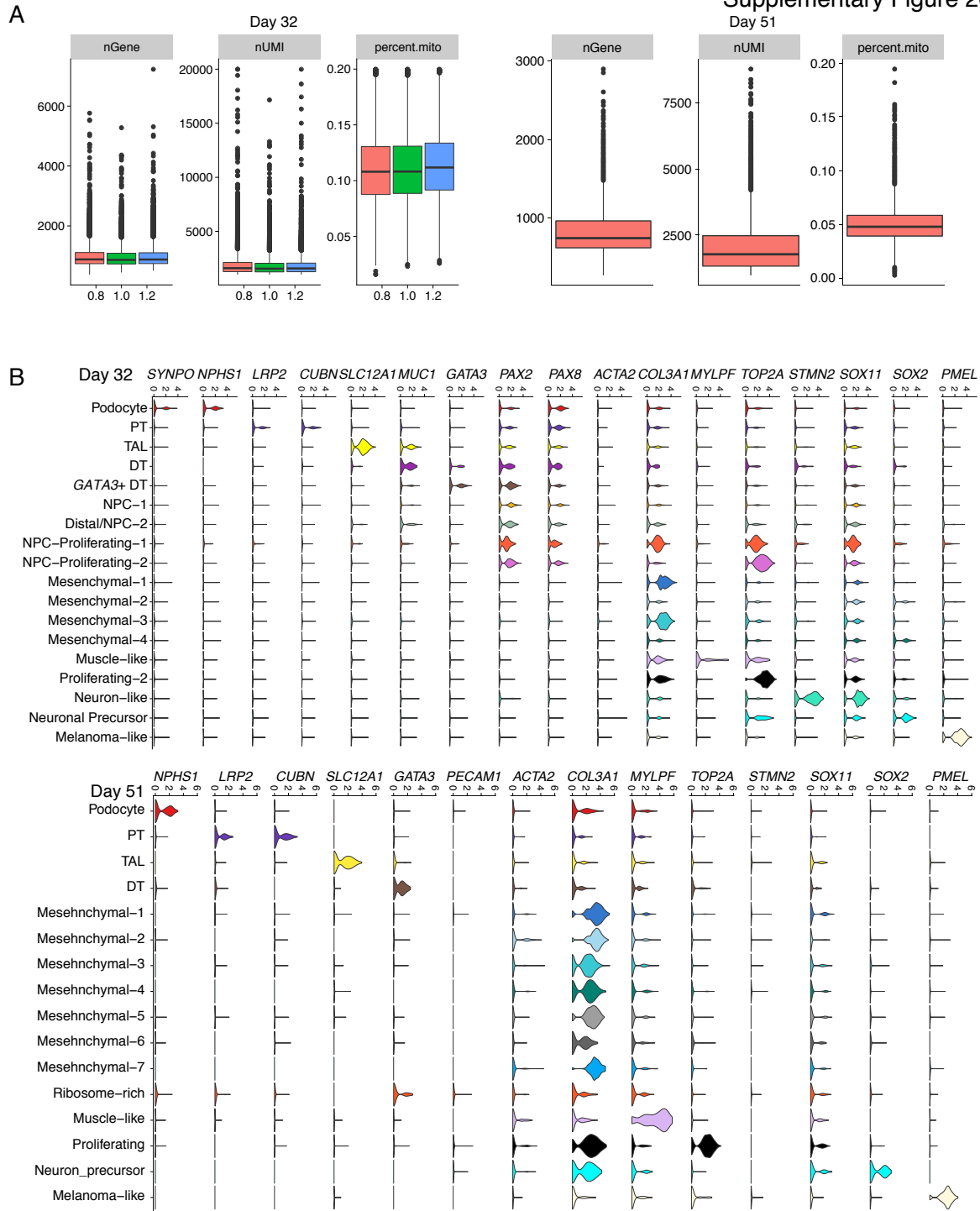
C



Supplementary Figure 19. Expression of monogenic causes of hereditary glomerular diseases in appropriate nephron epithelial cell types suggests utility of kidney organoids for understanding genetic kidney diseases.

Heat map comparison of gene expression in organoids ((A) D15, (B) D29) and (C) human adult of hereditary glomerular disease-causing genes in kidney epithelial cell clusters across 4 iPSC lines.

Supplementary Figure 20

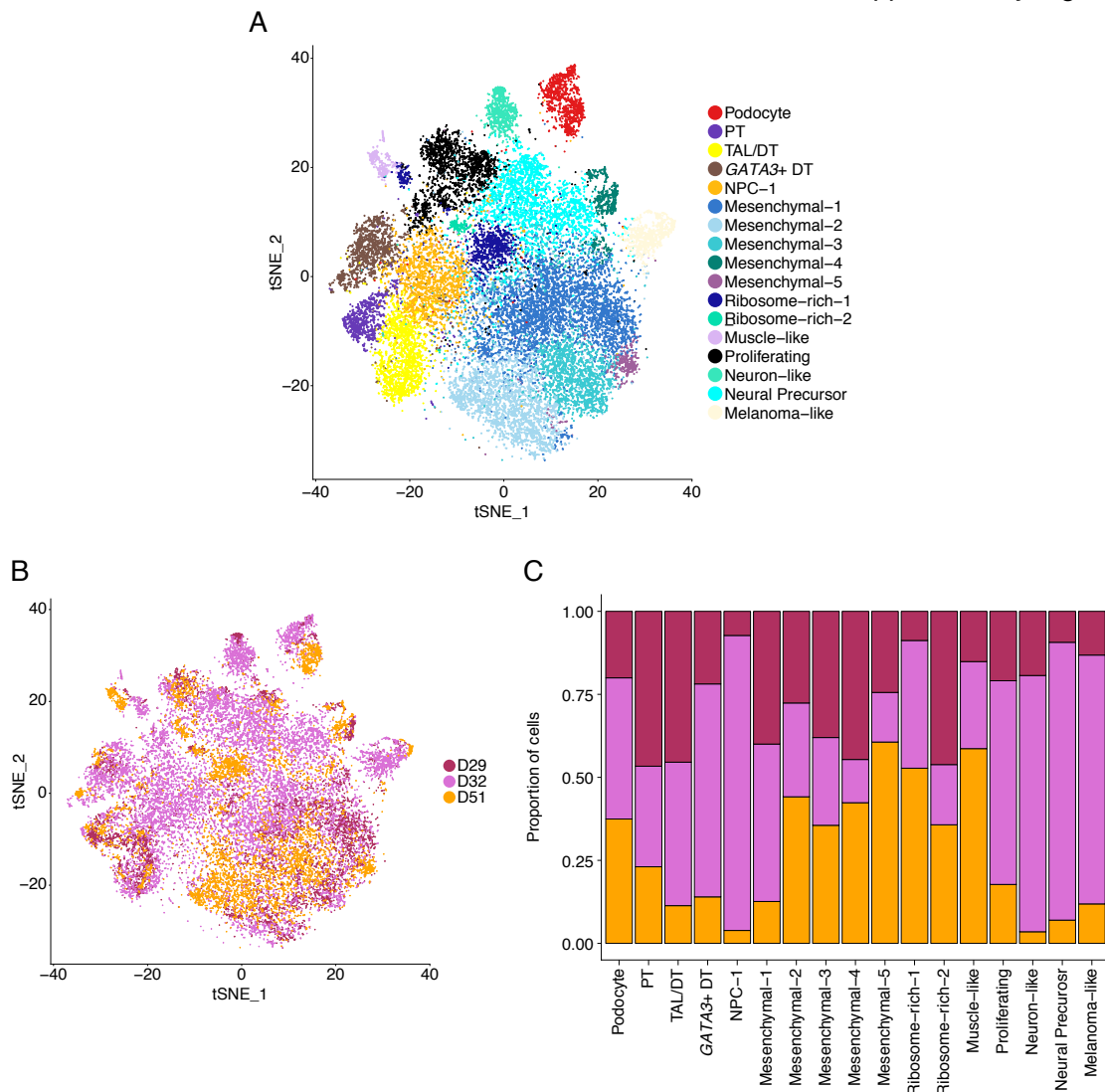


Supplementary Figure 20. Expression of cell type-specific differentially enriched genes in organoids in prolonged culture.

(A) Quality control summaries of D32 and D51 control organoids. The center line of the boxplots indicates the median, and the bottom and top lines of the box indicate the first and third quartiles respectively of the data points. Outliers are indicated as dots beyond the whiskers; whiskers

stretch up to $\pm 1.5 \times \text{IQR}$ on both sides. (B) Violin plot of single cells from D32 (top row) and D51 (bottom row) control organoids with gene expression of selected genes superimposed.

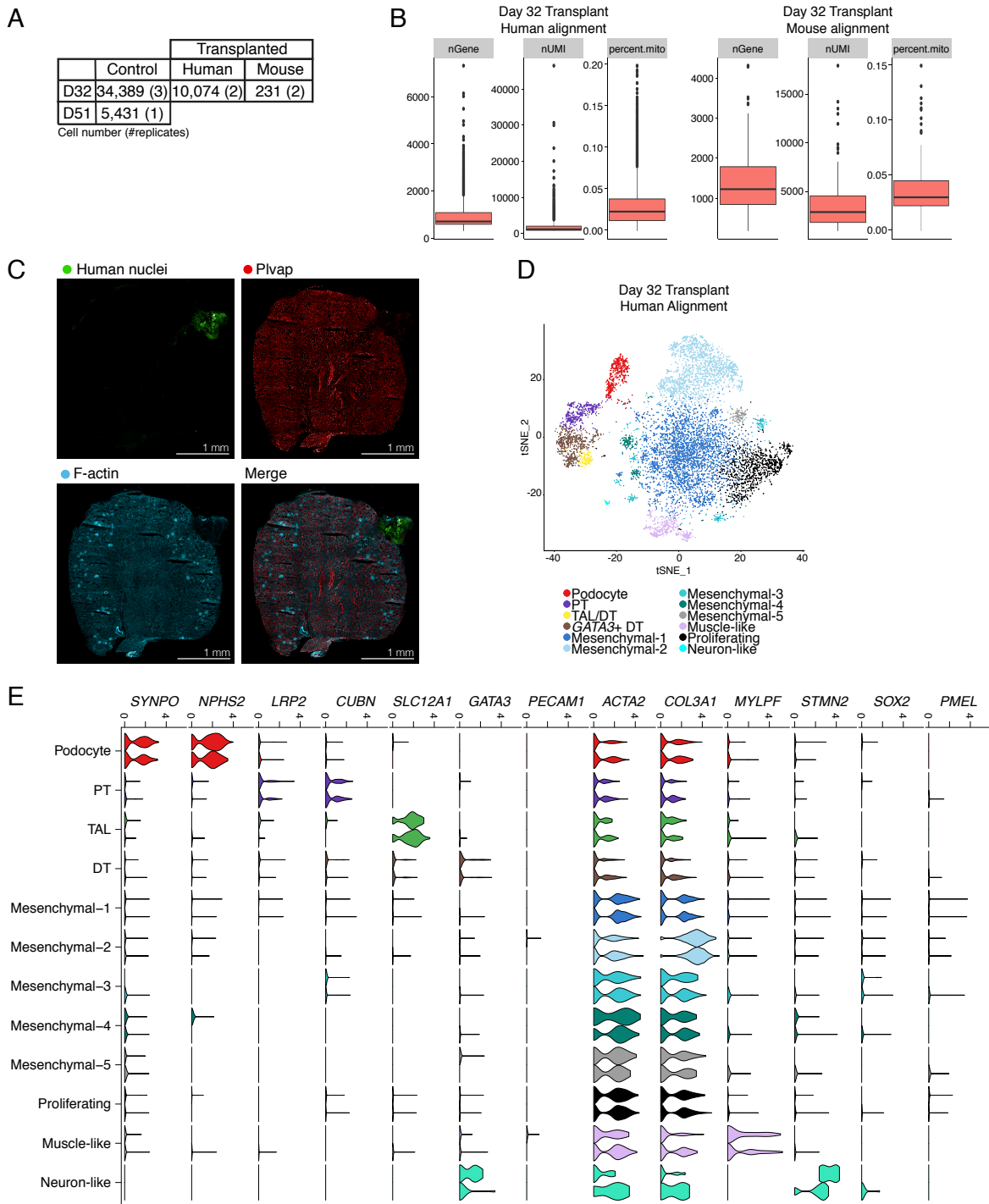
Supplementary Figure 21



Supplementary Figure 21. Integrated analysis of D29 (ThF), D32, and D51 control kidney organoid data.

(A) t-SNE plot of single cell transcriptomic profiles with cluster color annotations; (B) t-SNE plot of single cell transcriptomic profiles with sample origin color annotations; (C) Proportion plots of sample contribution per cluster.

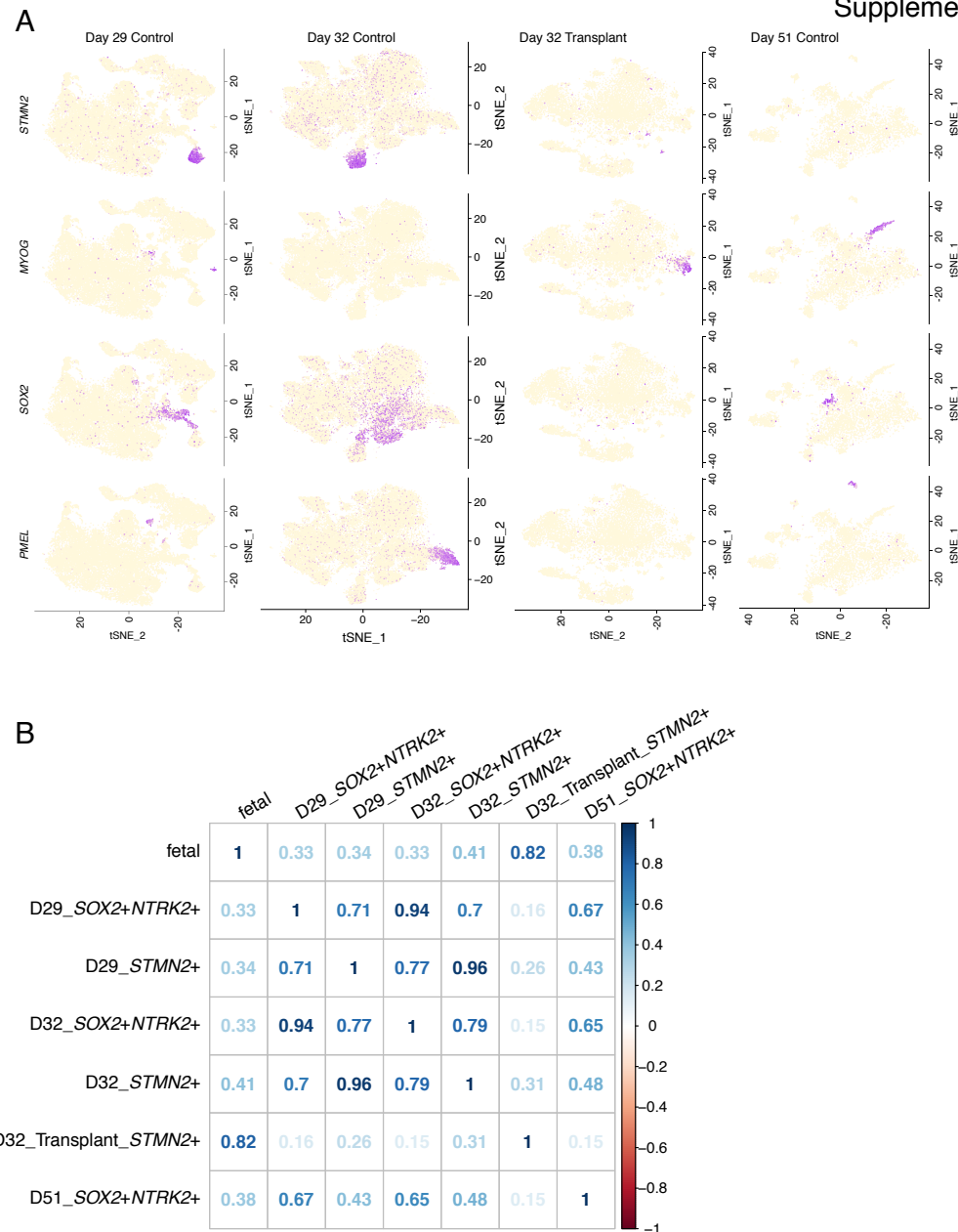
Supplementary Figure 22



Supplementary Figure 22. Single cell analysis of kidney subcapsular transplantation of organoids.

(A) Table of cell numbers from D32 cultured and transplanted organoids. (B) Quality control (QC) summaries of D32 transplanted kidney organoids from alignment to the combined human and mouse transcriptomes for (left) human and (right) mouse cells. The center line of the boxplots indicates the median, and the bottom and top lines of the box indicate the first and third quartiles respectively of the data points. Outliers are indicated as dots beyond the whiskers; whiskers stretch up to $+1.5 \times \text{IQR}$ on both sides. Data points represent QC summaries as indicated. (C) Immunofluorescence staining of D51 transplanted kidney organoids for human nuclei, mouse endothelial cells (Plvap), and cytoskeleton (F-actin). (D) t-SNE plot of human cells from D32 transplanted kidney organoids. (E) Violin plot of gene expression of canonical cluster markers in single cells from D32 transplanted organoids (human). Y-axis annotations represent clusters. Each violin per cluster represents a transplant replicate.

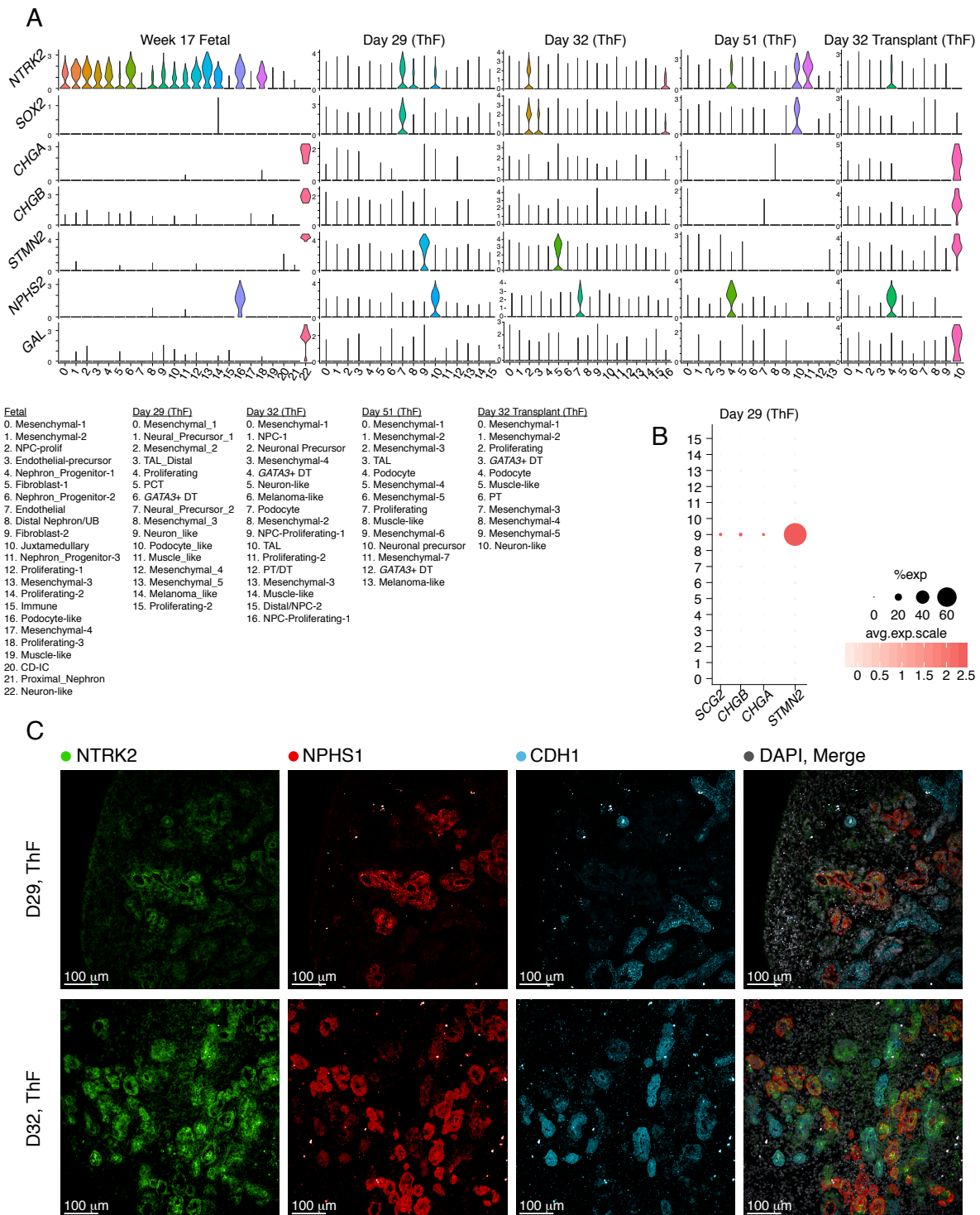
Supplementary Figure 23



Supplementary Figure 23. Off-target SOX2+ neuronal- and PMEL+ melanoma-like off-target cells reduced in transplanted organoids.

(A) t-SNE plot of single cells from *in vitro* (D29 and D32, and prolonged culture D51) and transplanted organoids with expression of off-target gene markers (*PMEL* [melanoma-like], *SOX2* [neuronal precursor], *MYOG* [muscle-like], *STMN2* [neuronal]). The colors indicate the range of expression from low (off-white) to high (purple). (B) Spearman correlation plot indicates that *STMN2*+ cells in transplanted organoids correlate most ($\rho = 0.82$) with fetal kidney, in contrast to organoids grown *in vitro*.

Supplementary Figure 24



Supplementary Figure 24. Transplanted organoids show similar expression of neuronal genes to second trimester fetal kidneys. (A) Violin plots of clusters from D29 and D32 controls, D51 prolonged culture and D32 transplanted showing expression of specific genes of interest. *NTRK2* is abundantly co-expressed with *NPHS2* (podocyte) in fetal kidney and across all organoids. The *STMN2+* neuronal cluster in fetal kidney is enriched in *CHGA*, *CHGB* and *GAL*, and this pattern of gene expression is uniquely recapitulated in D32 transplant organoids, but not in organoids grown *in vitro*. (B) Dot plot indicates expression of *CHGA* and *CHGB* was detectable in a small number of cells in D29 *STMN2+* cells. (C) Immunofluorescence staining of D29 and D32 control kidney organoids for *NTRK2*, podocytes (*NPHS1*), and distal tubules (*CDH1*).

Supplementary Table 1. Table of canonical markers for kidney (organoids and human)

Kidney compartment		Canonical Markers used for identification	
		Organoid	Human
Podocyte (1-5)	NPHS2, SYNPO,WT1	NPHS1, NPHS2, SYNPO, WT1, PODXL	
Proximal Tubule (1-4)	CUBN, LRP2,AQP1	CUBN, LRP2,AQP1, SLC7A3, SLC22A7	
Thick Ascending Limb (1-4)	SLC12A1	SLC12A1, UMOD	
Distal Convoluted Tubule (1-4)	-	SLC12A3, MUC1, CDH1	
Distal Nephron (3,4)	CDH1	-	
Ureteric Bud (1,2,7-10)		GATA3, RET, GFRA1, WNT11, ETV4, ETV5	
Collecting Duct – Principal Cells (1-3,6)	-	AQP2, SCNN1B, SCNN1G	
Collecting Duct – Intercalated Cells (1-3,6)		SLC4A9, ATP6V0D2	
Collecting Duct – alpha Intercalated Cells (1-3,6)	-	SLC4A1, KIT	
Collecting Duct – beta Intercalated Cells (1-3,6)	-	SLC26A4, INSRR	
Mesenchymal/vascular smooth muscle	COL3A1, MEIS2, MEIS1 [3,4]	ACTA2 [7]	
Mesenchymal/fibroblast		COL3A1	
Endothelial Cell (1,2,3,5,8,9)	PECAM1	PECAM1, KDR, FLT1, EMCN	Pecam1, Kdr, Flt1, Emcn
Fenestrated Endothelial Cell (10)	-	PECAM1, PLVAP	Pecam1, Plvap
Immune Cells (2)	-	PTPRC	

Other	Organoid
Epithelial (11)	EPCAM
Neuronal (3)	STMN2, SOX11
Neuronal (progenitor) (12,13)	SOX2
Muscle (3)	MYOG, MYLPF
Melanoma-like (3)	PMEL

Other (14-17)	Organoid
Nephron Progenitor Cells (Distal)	POU3F3, PAX2, LHX1, IRX3
Nephron Progenitor Cells (Proximal)	WT1, FOXC2, NOTCH2

Supplementary Table 2. Table of data-driven markers from D29 and D15

Organoid Stage	Kidney Cell	Data-driven Marker
D15	Podocyte	CLDN5
		SOST
		SPARC
		BST2
D29	Proximal Tubule (Proximal-distal gradient)	APOE
	Distal Nephron	WFDC2
		MAL
		DEFB1

Supplementary Table 3. Table of cell types and compartments

Putative_Cell_Types	Compartment
Endothelial Cells	Endothelial
Distal Nephron	Nephron
Nephron Progenitor Cells	Nephron
Podocyte	Nephron
Proximal Convoluted Tubule	Nephron
Thick Ascending Limb	Nephron
Mesenchymal Cells-1	Mesenchymal
Mesenchymal Cells-2	Mesenchymal
Mesenchymal Cells-3	Mesenchymal
Mesenchymal Cells-4	Mesenchymal
Mesenchymal Cells-5	Mesenchymal
Mesenchymal Cells-6	Mesenchymal
Mesenchymal Cells-7	Mesenchymal
Mesenchymal Cells-8	Mesenchymal
Proliferating	Mesenchymal
Muscle-like-1	Offtarget
Muscle-like-2	Offtarget
Neuron-like	Offtarget
Neuronal precursor	Offtarget
Melanoma	Offtarget

Supplementary Table 4. Table of developmental programs (14-17).

Ureteric Bud	RET, WNT9B, LHX1, ETV4, ETV5, WNT11, SPRY1, FGF9, GATA3, GFR1A
Metanephric Mesenchyme	OSR1, SALL1, WT1, EYA1, HOXD11, CITED1, PAX2, SIX1, SIX2, GDNF
Cap Mesenchyme	GDNF, PAX2, WT1, SIX2, CITED1, EYA1, WNT4
Pretubular aggregate	WNT4, LHX1
Renal Vesicle – distal	PAX2, LHX1, IRX3 (BRN1), LHX1
Renal Vesicle – Proximal	NOTCH2
Renal Vesicle – Glomerulus	FOXC2, WT1, VEGF

Supplemental References

1. Park, J. *et al.* Single-cell transcriptomics of the mouse kidney reveals potential cellular targets of kidney disease. *Science (80-.)* **360**, 758–763 (2018).
2. Wu, H., Kirita, Y., Donnelly, E. L. & Humphreys, B. D. Advantages of Single-Nucleus over Single-Cell RNA Sequencing of Adult Kidney: Rare Cell Types and Novel Cell States Revealed in Fibrosis. *J. Am. Soc. Nephrol.* **30**, 23–32 (2019).
3. Wu, H. *et al.* Comparative Analysis and Refinement of Human PSC-Derived Kidney Organoid Differentiation with Single-Cell Transcriptomics. *Cell Stem Cell* **23**, 869–881.e8 (2018).
4. Takasato, M. *et al.* Kidney organoids from human iPS cells contain multiple lineages and model human nephrogenesis. *Nature* **526**, 564–568 (2015).
5. Karaikos, N. *et al.* A Single-Cell Transcriptome Atlas of the Mouse Glomerulus. *J. Am. Soc. Nephrol.* **29**, 2060–2068 (2018).
6. Chen, L. *et al.* Transcriptomes of major renal collecting duct cell types in mouse identified by single-cell RNA-seq. *Proc. Natl. Acad. Sci.* **114**, E9989–E9998 (2017).
7. Xie, T. *et al.* Single-Cell Deconvolution of Fibroblast Heterogeneity in Mouse Pulmonary Fibrosis. *Cell Rep.* **22**, 3625–3640 (2018).
8. Lukowski, S. W. *et al.* Single-Cell Transcriptional Profiling of Aortic Endothelium Identifies a Hierarchy from Endovascular Progenitors to Differentiated Cells. *Cell Rep.* **27**, 2748–2758.e3 (2019).
9. Kalluri, A. S. *et al.* Single Cell Analysis of the Normal Mouse Aorta Reveals Functionally Distinct Endothelial Cell Populations. *Circulation CIRCULATIONAHA.118.038362* (2019). doi:10.1161/CIRCULATIONAHA.118.038362
10. Stan, R. V. *et al.* The Diaphragms of Fenestrated Endothelia: Gatekeepers of Vascular Permeability and Blood Composition. *Dev. Cell* **23**, 1203–1218 (2012).
11. Phipson, B. *et al.* Evaluation of variability in human kidney organoids. *Nat. Methods* **16**, 79–87 (2019).
12. Graham, V., Khudyakov, J., Ellis, P. & Pevny, L. SOX2 functions to maintain neural progenitor identity. *Neuron* **39**, 749–765 (2003).
13. Ellis, P. *et al.* SOX2, a persistent marker for multipotential neural stem cells derived from embryonic stem cells, the embryo or the adult. *Dev. Neurosci.* **26**, 148–65
14. Little, M. H. & McMahon, A. P. Mammalian kidney development: Principles, progress, and projections. *Cold Spring Harb. Perspect. Biol.* **4**, 3 (2012).
15. Sharma, R., Sanchez-Ferraz, O. & Bouchard, M. Pax genes in renal development, disease and regeneration. *Semin. Cell Dev. Biol.* **44**, 97–106 (2015).
16. Sirin, Y. & Susztak, K. Notch in the kidney: development and disease. *J. Pathol.* **226**, 394–403 (2012).
17. Krause, M., Rak-Raszewska, A., Pietilä, I., Quaggin, S. & Vainio, S. Signaling during Kidney Development. *Cells* **4**, 112–132 (2015).
18. Akchurin, O. & Reidy, K. J. Genetic causes of proteinuria and nephrotic syndrome: Impact on podocyte pathobiology. *Pediatr. Nephrol.* **30**, 221–233 (2015).
19. Wenderfer, S. E. & Gaut, J. P. Glomerular Diseases in Children. *Adv. Chronic Kidney Dis.* **24**, 364–371 (2017).
20. Dillman, J. R., Trout, A. T., Smith, E. A. & Towbin, A. J. Hereditary Renal Cystic Disorders: Imaging of the Kidneys and Beyond. *Radiographics* **37**, 924–946 (2017).
21. Capone, V. P., Morello, W., Taroni, F. & Montini, G. Genetics of Congenital Anomalies of the Kidney and Urinary Tract: The Current State of Play. *Int. J. Mol. Sci.* **18**, (2017).
22. Vivante, A. & Hildebrandt, F. Exploring the genetic basis of early-onset chronic kidney disease. *Nat. Rev. Nephrol.* **12**, 133–146 (2016).
23. Ware, S. M., Aygun, M. G.- & Hildebrandt, F. Spectrum of Clinical Diseases Caused By Disorders of Primary Cilia. *Proc. Am. Thorac. Soc.* **8**, 444–450 (2011).

24. Hildebrandt, F. Genetic kidney diseases. *Lancet (London, England)* **375**, 1287–95 (2010).
25. Warejko, J. K. *et al.* Whole exome sequencing of patients with steroid-resistant nephrotic syndrome. *Clin. J. Am. Soc. Nephrol.* **13**, 53–62 (2018).
26. Brown, E. J., Pollak, M. R. & Barua, M. Genetic testing for nephrotic syndrome and FSGS in the era of next-generation sequencing. *Kidney Int.* **85**, 1030–1038 (2014).
27. Yu, H. *et al.* A role for genetic susceptibility in sporadic focal segmental glomerulosclerosis. *J. Clin. Invest.* **126**, 1067–1078 (2016).
28. Ashraf, S. *et al.* Mutations in six nephrosis genes delineate a pathogenic pathway amenable to treatment. *Nat. Commun.* **9**, 1960 (2018).